


Higher-order corrections to spin-orbit and spin-spin tensor interactions in hydrogen molecular ions: Theory and application to H_2^+

Mohammad Haidar^{1,*}, Vladimir I. Korobov², Laurent Hilico^{1,3}, and Jean-Philippe Karr^{1,3}

¹Laboratoire Kastler Brossel, Sorbonne Université, CNRS, ENS-Université PSL, Collège de France, 4 place Jussieu, F-75005 Paris, France

²Bogoliubov Laboratory of Theoretical Physics, Joint Institute for Nuclear Research, Dubna 141980, Russia

³Université d'Evry-Val d'Essonne, Université Paris-Saclay, Boulevard François Mitterrand, F-91000 Evry, France

 (Received 4 July 2022; accepted 19 August 2022; published 29 August 2022)

We consider higher-order corrections to hyperfine coefficients related to the spin-orbit and spin-spin tensor interactions in hydrogen molecular ions. The $m\alpha^7 \ln(\alpha)$ -order radiative correction is derived in the NRQED framework. We present complete numerical calculations, including as well the $m\alpha^6$ -order relativistic correction, for the case of H_2^+ . The theoretical uncertainty is reduced by more than one order of magnitude with respect to the Breit-Pauli level, down to a few ppm. We also compare our results with available rf spectroscopy data.

DOI: [10.1103/PhysRevA.106.022816](https://doi.org/10.1103/PhysRevA.106.022816)

I. INTRODUCTION

In recent years, precision spectroscopy of hydrogen molecular ions has established itself as a fruitful direction for fundamental metrology. Rovibrational transition frequencies in HD^+ have been measured with very high accuracies [1,2] and compared with theoretical predictions [3] to obtain improved determinations of the proton-electron mass ratio or constrain hypothetical interactions beyond the Standard Model [4]. In these works, accurate predictions of the hyperfine structure have been used to extract a “spin-averaged” transition frequency from the measured hyperfine components. Discrepancies between theory and experiments have been observed in the hyperfine splitting of the rovibrational lines [5,6], which in some cases increases the uncertainty of rovibrational transition frequencies [2,7]. This makes it highly desirable to improve further the hyperfine structure theory in hydrogen molecular ions.

The theory of the leading hyperfine interaction, namely, the “Fermi” spin-spin contact interaction that gives rise to the main (~ 1 GHz) splitting in HD^+ and *ortho*- H_2^+ , has been recently improved [6,8]. The next step consists in improving the next largest hyperfine coefficients, related to the electronic spin-orbit and spin-spin tensor (dipolar) interactions [9,10]. It is worth noting that the spin-orbit and spin-spin tensor interactions, being essentially free of nuclear finite-size and structure corrections, allow for more precise tests of the theory with respect to the contact interaction. In Ref. [5] we derived the effective Hamiltonian for relativistic corrections of order $m\alpha^6$ in the hydrogen molecular ions, following the nonrelativistic QED (NRQED) approach that had been previously validated

by applying it to the hyperfine splitting of the $2P$ state in hydrogen [11]. This allowed us to get improved values of the spin-orbit coefficient for a few states [5]. In this work, we improve the theory further by deriving the radiative correction at the following order $m\alpha^7 \ln \alpha$.

We then present extensive numerical calculations of the spin-orbit and spin-spin tensor coefficients in the slightly simpler case of H_2^+ , whereas HD^+ will be considered in a forthcoming publication. There are several motivations to study the hyperfine structure specifically in H_2^+ . Recent efforts and proposals towards high-resolution laser spectroscopy of this ion [12–14] offer opportunities to test the theory; accurate theoretical predictions of the hyperfine splitting are also likely to be required to extract spin-averaged transition frequencies, similarly to HD^+ [1,2]. Moreover, H_2^+ is of high astrophysical importance due to its role in the formation of H_3^+ . This has made its radio-astronomical detection, using, e.g., hyperfine transitions analogous to the 21-cm line in atomic hydrogen, a long-standing goal [15–17]. Interest in H_2^+ is further enhanced by prospects of experimental studies on the antihydrogen molecular ion \bar{H}_2^- , aimed at performing improved tests of the CPT symmetry [18]; some of these tests could be performed through measurements of hyperfine-Zeeman transitions. Finally, a few hyperfine intervals that are essentially independent from the “Fermi” coefficients have been measured with very high precision ($\sim 10^{-7}$) [19], thus providing a stringent test of theory for the spin-orbit and spin-spin tensor interactions.

II. NRQED HAMILTONIAN

For calculation of $m\alpha^7$ -order corrections, a more complete version of the NRQED Hamiltonian used in our previous works [5,11] is required. Namely, its coefficients should be determined up to first order in α by matching NRQED and QED scattering amplitudes [20–22]. Writing only the terms that are relevant for the present consideration, the NRQED Hamiltonian has the form

*Present address: Sorbonne Université, Laboratoire de Chimie Théorique (LCT), 4 place Jussieu, F-75005 Paris, France; Sorbonne Université, CNRS, Université Paris Cité, Laboratoire Jacques-Louis Lions (LJLL), 4 place Jussieu, F-75005 Paris, France; TotalEnergies, Tour Coupole, 2 Pl. Jean Millier, F-92078 Paris la Défense, France.

$$\begin{aligned}
 H_I = & eA_0 + \frac{\boldsymbol{\pi}^2}{2m} - \frac{\boldsymbol{\pi}^4}{8m^3} - c_F \frac{e}{2m} \boldsymbol{\sigma} \cdot \mathbf{B} - c_D \frac{e}{8m^2} [\boldsymbol{\partial} \cdot \mathbf{E}] + c_S \frac{e}{8m^2} \boldsymbol{\sigma} \cdot (\boldsymbol{\pi} \times \mathbf{E} - \mathbf{E} \times \boldsymbol{\pi}) \\
 & + c_W \frac{e}{8m^3} \{\boldsymbol{\pi}^2, \boldsymbol{\sigma} \cdot \mathbf{B}\} - c_{q^2} \frac{e}{8m^3} \boldsymbol{\sigma} \cdot [\Delta \mathbf{B}] + c_{p'p} \frac{e}{8m^3} (\boldsymbol{\sigma} \cdot \boldsymbol{\pi} \mathbf{B} \cdot \boldsymbol{\pi} + \boldsymbol{\pi} \cdot \mathbf{B} \boldsymbol{\sigma} \cdot \boldsymbol{\pi}) + c_M \frac{e}{8m^3} \{\boldsymbol{\pi}, [\boldsymbol{\partial} \times \mathbf{B}]\} \\
 & + c_{X_1} \frac{ie}{128m^4} [\boldsymbol{\pi}^2, (\boldsymbol{\pi} \cdot \mathbf{E} + \mathbf{E} \cdot \boldsymbol{\pi})] + c_{X_2} \frac{e}{64m^4} \{\boldsymbol{\pi}^2, [\boldsymbol{\partial} \cdot \mathbf{E}]\} - c_{X_3} \frac{e}{8m^4} [\Delta [\boldsymbol{\partial} \cdot \mathbf{E}]] \\
 & - c_{Y_1} \frac{e}{64m^4} \{\boldsymbol{\pi}^2, \boldsymbol{\sigma} \cdot (\boldsymbol{\pi} \times \mathbf{E} - \mathbf{E} \times \boldsymbol{\pi})\} + c_{Y_2} \frac{ie}{4m^4} \epsilon_{ijk} \sigma^i \pi^j [\boldsymbol{\partial} \cdot \mathbf{E}] \pi^k, \tag{1}
 \end{aligned}$$

where $\boldsymbol{\pi} = \mathbf{p} - e\mathbf{A}$, $\mathbf{E} = -\partial_t \mathbf{A} - \nabla A_0$, $\mathbf{B} = \nabla \times \mathbf{A}$, $[X, Y] = XY - YX$, and $\{X, Y\} = XY + YX$. Square brackets around quantities imply that derivatives act only within the bracket [this notation applies only to Eq. (1) and is not used in the following].

The above expression differs from Eq. (1) of [22], which is complete up to the order $1/m^4$, in several details. First, we have omitted terms involving the coefficients c_{X_4} and $c_{X_7} - c_{X_{12}}$, which contribute only at orders $m\alpha^8$ and above, and the two-photon (seagull) terms involving c_{A_1} and c_{A_2} , since for the corrections we aim to calculate it is sufficient to perform a matching of one-photon scattering amplitudes. Second, the terms involving the coefficients c_{W_1} and c_{W_2} have been reformulated by introducing the coefficients c_W and c_{q^2} , as done in [20,23]. In a similar way, we have reformulated the terms involving c_{X_5} and c_{X_6} by introducing c_{Y_1} and c_{Y_2} . The reason behind these transformations is to get simpler expressions for the NRQED effective potentials. Finally, for convenience we have changed the definitions of $c_{X_1} - c_{X_3}$ by introducing numerical prefactors in the corresponding terms.

For the following calculations, $\boldsymbol{\pi}$ can be replaced by \mathbf{p} in the last three lines because the terms involving \mathbf{A} contribute only at higher orders.

The QED scattering amplitude at tree level for a static scalar field $A_0(\mathbf{q})$ is

$$A_E^{\text{QED}}(p, p') = -iA_0 J^0(p, p'), \tag{2}$$

where p, p' are the four-momenta of the incident and scattered particle, and J is the charge-current density operator, which is

written in terms of the Dirac and Pauli form factors $F_1(q^2)$ and $F_2(q^2)$ (with $\mathbf{q} = \mathbf{p}' - \mathbf{p}$):

$$J^\mu = ie \bar{u}(p') \left(\gamma^\mu F_1(q^2) + \frac{i\kappa}{2m} \sigma^{\mu\nu} q_\nu F_2(q^2) \right) u(p). \tag{3}$$

Here κ is the particle's anomalous magnetic moment, and $u(p), u(p')$ are on-shell Dirac spinors. Using the nonrelativistic normalization condition $u^*(p)u(p) = 1$, a Dirac spinor can be expressed in terms of a Schrödinger-Pauli spinor $\psi(p)$ as

$$u(p) = \sqrt{\frac{E_p + m}{2E_p}} \begin{pmatrix} \psi(p) \\ \frac{\boldsymbol{\sigma} \cdot \mathbf{p}}{E_p + m} \psi(p) \end{pmatrix}, E_p = \sqrt{m^2 + \mathbf{p}^2}. \tag{4}$$

It can then be expanded in powers of \mathbf{p}^2/m^2 :

$$u(p) \approx \begin{pmatrix} \left[1 - \frac{\mathbf{p}^2}{8m^2} + \frac{11\mathbf{p}^4}{128m^4} + \dots \right] \psi \\ \frac{\boldsymbol{\sigma} \cdot \mathbf{p}}{2m} \left[1 - \frac{3\mathbf{p}^2}{8m^2} + \dots \right] \psi \end{pmatrix}. \tag{5}$$

The form factors can also be expanded as

$$F_1(q^2) = \bar{F}_1 - \bar{F}'_1 \frac{\mathbf{q}^2}{m^2} + \bar{F}''_1 \frac{\mathbf{q}^4}{m^4} + \dots, \tag{6}$$

$$F_2(q^2) = \bar{F}_2 - \bar{F}'_2 \frac{\mathbf{q}^2}{m^2} + \dots \tag{7}$$

with $\bar{F}_1 = \bar{F}_2 = 1$ for an electron. Using Eqs. (2)–(3) and (5)–(7), one gets the following expansion of the QED scattering amplitude:

$$\begin{aligned}
 A_E^{\text{QED}}(p, p') = & \psi^*(p') eA_0 \left[\bar{F}_1 - \frac{\mathbf{q}^2}{8m^2} (\bar{F}_1 + 2\kappa \bar{F}_2 + 8\bar{F}'_1) + i \frac{\boldsymbol{\sigma} \cdot (\mathbf{q} \times \mathbf{p})}{4m^2} (\bar{F}_1 + 2\kappa \bar{F}_2) \right. \\
 & + \frac{\mathbf{q}^4}{8m^4} (\bar{F}'_1 + 2\kappa \bar{F}'_2 + 8\bar{F}''_1) - i \frac{\boldsymbol{\sigma} \cdot (\mathbf{q} \times \mathbf{p}) \mathbf{q}^2}{4m^4} (\bar{F}'_1 + 2\kappa \bar{F}'_2) + \frac{\mathbf{q}^2 (p'^2 + p^2)}{64m^4} (3\bar{F}_1 + 4\kappa \bar{F}_2) \\
 & \left. + \frac{(p'^2 - p^2)^2}{128m^4} (5\bar{F}_1 + 4\kappa \bar{F}_2) - i \frac{\boldsymbol{\sigma} \cdot (\mathbf{q} \times \mathbf{p}) (p'^2 + p^2)}{32m^4} (3\bar{F}_1 + 4\kappa \bar{F}_2) + \dots \right] \psi(p). \tag{8}
 \end{aligned}$$

Similarly, for a vector field $\mathbf{A}(\mathbf{q})$, the scattering amplitude

$$A_M^{\text{QED}}(p, p') = -iA_\mu J^\mu(p, p') \tag{9}$$

can be expanded as follows:

$$\begin{aligned}
A_M^{\text{QED}}(p, p') = \psi^*(p')e\mathbf{A} \cdot & \left[-\frac{(\mathbf{p}' + \mathbf{p})}{2m}\bar{F}_1 - i\frac{(\boldsymbol{\sigma} \times \mathbf{q})}{2m}(\bar{F}_1 + \kappa\bar{F}_2) + \frac{\mathbf{q}^2(\mathbf{p}' + \mathbf{p})}{16m^3}(8\bar{F}'_1 + \kappa\bar{F}_2) + \frac{(\mathbf{p}' + \mathbf{p})(p'^2 + p^2)\bar{F}_1}{8m^3} \right. \\
& + \frac{\mathbf{q}(p'^2 - p^2)}{16m^3}(\bar{F}_1 - \kappa\bar{F}_2) + i\frac{(\boldsymbol{\sigma} \times \mathbf{q})(p'^2 + p^2)}{8m^3}\bar{F}_1 + i\frac{[\boldsymbol{\sigma} \times (\mathbf{p}' + \mathbf{p})](p'^2 - p^2)}{16m^3}\bar{F}_1 \\
& \left. + i\frac{(\boldsymbol{\sigma} \cdot \mathbf{p}')(\mathbf{p} \times \mathbf{q}) + (\boldsymbol{\sigma} \cdot \mathbf{p})(\mathbf{p}' \times \mathbf{q})}{8m^3}\kappa\bar{F}_2 + i\frac{\mathbf{q}^2(\boldsymbol{\sigma} \times \mathbf{q})}{16m^3}(\kappa\bar{F}_2 + 8\bar{F}'_1 + 8\kappa\bar{F}'_2) \right] \psi(p). \quad (10)
\end{aligned}$$

The NRQED scattering amplitude is directly obtained from the Hamiltonian (1). For a scalar field one gets

$$\begin{aligned}
A_E^{\text{NRQED}}(p, p') = \psi^*(p')eA_0 \left[1 - c_D \frac{\mathbf{q}^2}{8m^2} + ic_S \frac{\boldsymbol{\sigma} \cdot [\mathbf{q} \times (\mathbf{p}' + \mathbf{p})]}{8m^2} + c_{X_1} \frac{(p'^2 - p^2)^2}{128m^4} + c_{X_2} \frac{(p'^2 + p^2)\mathbf{q}^2}{64m^4} + c_{X_3} \frac{\mathbf{q}^4}{8m^4} \right. \\
\left. - ic_{Y_1} \frac{(p'^2 + p^2)\boldsymbol{\sigma} \cdot [\mathbf{q} \times (\mathbf{p}' + \mathbf{p})]}{64m^4} + ic_{Y_2} \frac{\boldsymbol{\sigma} \cdot [\mathbf{q} \times (\mathbf{p}' + \mathbf{p})]\mathbf{q}^2}{8m^4} \right] \psi(p), \quad (11)
\end{aligned}$$

and for a vector field:

$$\begin{aligned}
A_M^{\text{NRQED}}(p, p') = \psi^*(p')e\mathbf{A} \cdot \left[-\frac{(\mathbf{p}' + \mathbf{p})}{2m} - ic_F \frac{(\boldsymbol{\sigma} \times \mathbf{q})}{2m} + \frac{(p'^2 + p^2)(\mathbf{p}' + \mathbf{p})}{8m^3} + ic_W \frac{(p'^2 + p^2)(\boldsymbol{\sigma} \times \mathbf{q})}{8m^3} + ic_{q^2} \frac{\mathbf{q}^2(\boldsymbol{\sigma} \times \mathbf{q})}{8m^3} \right. \\
\left. + ic_{p'p} \frac{(\boldsymbol{\sigma} \cdot \mathbf{p}')(\mathbf{p} \times \mathbf{q}) + (\boldsymbol{\sigma} \cdot \mathbf{p})(\mathbf{p}' \times \mathbf{q})}{8m^3} + c_M \frac{\mathbf{q}^2(\mathbf{p}' + \mathbf{p})}{8m^3} \right] \psi(p). \quad (12)
\end{aligned}$$

Matching Eq. (11) with Eq. (8) and Eq. (12) with Eq. (10) allows us to determine the coefficients of the NRQED Hamiltonian. Note that the last term in the third line of Eq. (10) does not appear in the corresponding NRQED expression (12), because it is gauge dependent and thus does not contribute to the scattering amplitude. Our final result is

$$\begin{aligned}
c_F = \bar{F}_1 + \kappa\bar{F}_2, & \quad c_D = \bar{F}_1 + 2\kappa\bar{F}_2 + 8\bar{F}'_1, & \quad c_S = \bar{F}_1 + 2\kappa\bar{F}_2, \\
c_W = \bar{F}_1, & \quad c_{q^2} = \frac{1}{2}(\kappa\bar{F}_2 + 8\bar{F}'_1 + 8\kappa\bar{F}'_2), & \quad c_{p'p} = \kappa\bar{F}_2, \\
c_M = \frac{1}{2}(\kappa\bar{F}_2 + 8\bar{F}'_1), & \quad c_{X_1} = 5\bar{F}_1 + 4\kappa\bar{F}_2, & \quad c_{X_2} = 3\bar{F}_1 + 4\kappa\bar{F}_2, \\
c_{X_3} = \bar{F}'_1 + 2\kappa\bar{F}'_2 + 8\bar{F}''_1, & \quad c_{Y_1} = 3\bar{F}_1 + 4\kappa\bar{F}_2, & \quad c_{Y_2} = -(\bar{F}'_1 + 2\kappa\bar{F}'_2).
\end{aligned} \quad (13)$$

This can be compared with Ref. [22] with the help of the relationships

$$\begin{aligned}
c_W + c_{q^2} = c_{W_1}, & \quad c_{q^2} = c_{W_2}, \\
c_{Y_1} = 32c_{X_3}, & \quad -c_{Y_1} + 8c_{Y_2} = 32c_{X_6},
\end{aligned} \quad (14)$$

which are easily obtained using the equation $\mathbf{q}^2 = p'^2 + p^2 - 2\mathbf{p}' \cdot \mathbf{p}$. Our results are in agreement with those of Ref. [22], except for c_{X_1} and c_{X_3} . Note that these two coefficients do not depend on spin and therefore do not play any role in the interactions studied in this work. For the electron case, the first expansion coefficients of the form factors are

$$\bar{F}'_1 = \frac{\alpha}{3\pi} \left[\ln\left(\frac{m}{\lambda}\right) - \frac{3}{8} \right] + \dots, \quad \bar{F}''_1 = \frac{\alpha}{20\pi} \left[\ln\left(\frac{m}{\lambda}\right) - \frac{11}{12} \right] + \dots, \quad a_e \bar{F}'_2 = \frac{\alpha}{12\pi} + \dots, \quad (15)$$

where λ is a photon mass, and a_e is the electron's anomalous magnetic moment. The coefficients of the NRQED Hamiltonian are then

$$\begin{aligned}
c_F = 1 + a_e, & \quad c_D = 1 + 2a_e + \frac{8}{3} \frac{\alpha}{\pi} \left[\ln\left(\frac{m}{\lambda}\right) - \frac{3}{8} \right], & \quad c_S = 1 + 2a_e, \\
c_W = 1, & \quad c_{q^2} = \frac{a_e}{2} + \frac{4}{3} \frac{\alpha}{\pi} \left[\ln\left(\frac{m}{\lambda}\right) - \frac{1}{8} \right], & \quad c_{p'p} = a_e, \\
c_M = \frac{a_e}{2} + \frac{4}{3} \frac{\alpha}{\pi} \left[\ln\left(\frac{m}{\lambda}\right) - \frac{3}{8} \right], & \quad c_{X_1} = 5 + 4a_e, & \quad c_{X_2} = 3 + 4a_e, \\
c_{X_3} = \frac{\alpha}{\pi} \left[\frac{11}{15} \ln\left(\frac{m}{\lambda}\right) - \frac{13}{40} \right], & \quad c_{Y_1} = 3 + 4a_e, & \quad c_{Y_2} = -\frac{1}{3} \frac{\alpha}{\pi} \left[\ln\left(\frac{m}{\lambda}\right) + \frac{1}{8} \right].
\end{aligned} \quad (16)$$

It is important to note that logarithmic contributions can be immediately obtained by substituting the photon mass λ in the $\ln(m/\lambda)$ terms with the natural energy scale $m\alpha^2$ (see, e.g., [24]).

III. HYPERFINE STRUCTURE CORRECTIONS AT ORDERS $m\alpha^6$ AND $m\alpha^7 \ln(\alpha)$

A. Terms contributing at the order $m\alpha^6$

Effective potentials contributing to the spin-orbit and spin-spin tensor interactions can be obtained from the NRQED Hamiltonian, Eq. (1), using perturbation theory. For the $m\alpha^6$ order, this has been done in our previous work [5]. We recall these results before moving on to the corrections appearing at order $m\alpha^7 \ln(\alpha)$. We use natural relativistic units ($\hbar = c = 1$) and the following notations: \mathbf{s}_e is the electron spin, Z_1, Z_2 and M_1, M_2 are the nuclear charges and masses (here $Z_1 = Z_2 = 1, M_1 = M_2 = m_p$), $\mathbf{r}_a = \mathbf{r}_e - \mathbf{R}_a$ ($a = 1, 2$) is the position of the electron with respect to nucleus a , and $\mathbf{p}_e, \mathbf{P}_1, \mathbf{P}_2$ are the impulse operators for the electron and both nuclei, respectively.

We first list the corrections to the electronic spin-orbit interaction. The total energy correction can be written as

$$\Delta E_{so(6)} = \Delta E_{so(6)}^A + \Delta E_{so(6)}^B. \quad (17)$$

Here the first term is the first-order contribution, given by the expectation value of a $m\alpha^6$ -order effective Hamiltonian:

$$\begin{aligned} \Delta E_{so(6)}^A &= \langle H_{so(6)} \rangle, \\ H_{so(6)} &= c_W \mathcal{U}_W + c_{Y_1} \mathcal{U}_{Y_1} + c_S \mathcal{U}_{CM} + \mathcal{U}_{MM_N}, \\ \mathcal{U}_W &= \frac{Z_a}{4m^3 M_a} \left\{ p_e^2, \frac{1}{r_a^3} (\mathbf{r}_a \times \mathbf{P}_a) \right\} \cdot \mathbf{s}_e, \\ \mathcal{U}_{Y_1} &= -\frac{Z_a}{16m^4} \left\{ p_e^2, \frac{1}{r_a^3} (\mathbf{r}_a \times \mathbf{p}_e) \right\} \cdot \mathbf{s}_e, \\ \mathcal{U}_{CM} &= \frac{Z_a^2}{4m^2 M_a} \frac{1}{r_a^4} (\mathbf{r}_a \times \mathbf{P}_a) \cdot \mathbf{s}_e + \frac{Z_1 Z_2}{4m^2 M_1} \frac{1}{r_1 r_2^3} (\mathbf{r}_2 \times \mathbf{P}_1) \cdot \mathbf{s}_e \\ &\quad + \frac{Z_1 Z_2}{4m^2 M_2} \frac{1}{r_1^3 r_2} (\mathbf{r}_1 \times \mathbf{P}_2) \cdot \mathbf{s}_e \\ &\quad - \frac{Z_1 Z_2}{4m^2 M_a} \frac{1}{r_1^3 r_2^3} (\mathbf{r}_1 \times \mathbf{r}_2) (\mathbf{r}_a \cdot \mathbf{P}_a) \cdot \mathbf{s}_e, \\ \mathcal{U}_{MM_N} &= -\frac{Z_a^2}{2m^2 M_a} \frac{1}{r_a^4} (\mathbf{r}_a \times \mathbf{p}_e) \cdot \mathbf{s}_e, \end{aligned} \quad (18)$$

with implicit summation over $a = 1, 2$. $\langle \cdot \rangle$ denotes an expectation value with the nonrelativistic wave function ψ_0 . We have omitted retardation terms, which were considered in [5] and shown to be negligibly small. The second term of Eq. (17) is the second-order contribution, which arises from various terms of the Breit-Pauli Hamiltonian:

$$\begin{aligned} \Delta E_{so(6)}^B &= \Delta E_{so-H_B} + \Delta E_{so-ret} + \Delta E_{so-so}^{(1)}, \\ \Delta E_{so-H_B} &= 2 \langle H_{so} Q (E_0 - H_0)^{-1} Q H_B \rangle, \\ \Delta E_{so-ret} &= 2 \langle H_{so} Q (E_0 - H_0)^{-1} Q H_{ret} \rangle, \\ \Delta E_{so-so}^{(1)} &= \langle [H_{so} Q (E_0 - H_0)^{-1} Q H_{so}]^{(1)} \rangle, \end{aligned} \quad (19)$$

where H_0 and E_0 are, respectively, the nonrelativistic Hamiltonian and energy, and Q is a projection operator on a subspace orthogonal to ψ_0 . $A^{(k)}$ denotes the term of rank k in the decomposition of A as a sum of irreducible tensor operators. The involved terms of the Breit Pauli-Hamiltonian are

$$\begin{aligned} H_B &= -\frac{p_e^4}{8m^3} + \frac{Z_a \pi}{2m^2} \delta(\mathbf{r}_a), \\ H_{ret} &= \frac{Z_a}{2} \frac{p_e^i}{m} \left(\frac{\delta^{ij}}{r_a} + \frac{r_a^i r_a^j}{r_a^3} \right) \frac{P_a^j}{M_a}, \\ H_{so} &= \frac{Z_a(1+2a_e)}{2m^2} \frac{(\mathbf{r}_a \times \mathbf{p}_e) \cdot \mathbf{s}_e}{r_a^3} - \frac{Z_a(1+a_e)}{mM_a} \frac{(\mathbf{r}_a \times \mathbf{P}_a) \cdot \mathbf{s}_e}{r_a^3}. \end{aligned} \quad (20)$$

We now turn to the electron-nucleus spin-spin tensor interaction. Similarly, we have

$$\Delta E_{ss(6)}^{(2)} = \Delta E_{ss(6)}^{(2)A} + \Delta E_{ss(6)}^{(2)B}, \quad (21)$$

where the first term is the expectation value of a $m\alpha^6$ -order effective Hamiltonian:

$$\begin{aligned} \Delta E_{ss(6)}^{(2)A} &= \langle H_{ss(6)}^{(2)} \rangle, \\ H_{ss(6)}^{(2)} &= c_W \mathcal{U}_W^{(2)} + c_S \mathcal{U}_{CM}^{(2)}, \\ \mathcal{U}_W^{(2)} &= -\frac{1}{4m^2} \left\{ p_e^2, \frac{r_a^2 \boldsymbol{\mu}_e \cdot \boldsymbol{\mu}_a - 3(\boldsymbol{\mu}_e \cdot \mathbf{r}_a)(\boldsymbol{\mu}_a \cdot \mathbf{r}_a)}{r_a^5} \right\}, \\ \mathcal{U}_{CM}^{(2)} &= -\frac{Z_a}{6m} \frac{r_a^2 \boldsymbol{\mu}_e \cdot \boldsymbol{\mu}_a - 3(\boldsymbol{\mu}_e \cdot \mathbf{r}_a)(\boldsymbol{\mu}_a \cdot \mathbf{r}_a)}{r_a^6} \\ &\quad - \frac{1}{6m} \left[Z_2 \frac{(\mathbf{r}_1 \cdot \mathbf{r}_2) \boldsymbol{\mu}_e \cdot \boldsymbol{\mu}_1 - 3(\boldsymbol{\mu}_e \cdot \mathbf{r}_1)(\boldsymbol{\mu}_1 \cdot \mathbf{r}_2)}{r_1^3 r_2^3} \right. \\ &\quad \left. + Z_1 \frac{(\mathbf{r}_1 \cdot \mathbf{r}_2) \boldsymbol{\mu}_e \cdot \boldsymbol{\mu}_2 - 3(\boldsymbol{\mu}_e \cdot \mathbf{r}_2)(\boldsymbol{\mu}_2 \cdot \mathbf{r}_1)}{r_1^3 r_2^3} \right]. \end{aligned} \quad (22)$$

Here $\boldsymbol{\mu}_e$ and $\boldsymbol{\mu}_a$ are the electronic and nuclear magnetic moments. Neglecting the electron's anomalous magnetic moment, we get $\boldsymbol{\mu}_e = -(|e|/m)\mathbf{s}_e$. In H_2^+ , $\boldsymbol{\mu}_a = 2\mu_p \mu_N \mathbf{I}_a$, where μ_p is the proton's magnetic moment in units of the nuclear Bohr magneton μ_N , and \mathbf{I}_a the spin operator of nucleus a . The second-order contribution is

$$\begin{aligned} \Delta E_{ss(6)}^{(2)B} &= \Delta E_{ss-H_B}^{(2)} + \Delta E_{so-ss}^{(2)} + \Delta E_{so-soN}^{(2)}, \\ \Delta E_{ss-H_B}^{(2)} &= 2 \langle H_{ss}^{(2)} Q (E_0 - H_0)^{-1} Q H_B \rangle, \\ \Delta E_{so-ss}^{(2)} &= 2 \langle [H_{ss}^{(2)} Q (E_0 - H_0)^{-1} Q H_{so}]^{(2)} \rangle, \\ \Delta E_{so-soN}^{(2)} &= 2 \langle [H_{so} Q (E_0 - H_0)^{-1} Q H_{soN}]^{(2)} \rangle. \end{aligned} \quad (23)$$

It involves two additional terms of the Breit-Pauli Hamiltonian:

$$\begin{aligned} H_{ss}^{(2)} &= \left[\frac{\boldsymbol{\mu}_e \cdot \boldsymbol{\mu}_a}{r_a^3} - 3 \frac{(\boldsymbol{\mu}_e \cdot \mathbf{r}_a)(\boldsymbol{\mu}_a \cdot \mathbf{r}_a)}{r_a^5} \right] - \frac{8\pi\alpha}{3} \boldsymbol{\mu}_e \cdot \boldsymbol{\mu}_a \delta(\mathbf{r}_a), \\ H_{soN} &= \frac{1}{m} \frac{(\mathbf{r}_a \times \mathbf{p}_e) \cdot \boldsymbol{\mu}_a}{r_a^3} - \frac{1}{M_a} \left(1 - \frac{Z_a m_p I_a}{M_a \mu_a} \right) \frac{(\mathbf{r}_a \times \mathbf{P}_a) \cdot \boldsymbol{\mu}_a}{r_a^3}. \end{aligned} \quad (24)$$

We have changed our notations of the first-order terms with respect to Ref. [5] in order to clearly identify their link to

the terms of the NRQED Hamiltonian. \mathcal{U}_{CM} and \mathcal{U}_{MM_N} denote seagull terms with simultaneous exchange of a Coulomb and a magnetic photon (CM), and of two magnetic photons at the nucleus (MM_N). The correspondence with notations used in our earlier work [5] is the following:

$$\begin{aligned} \mathcal{U}_W &\leftrightarrow \mathcal{U}_{2b}, \quad \mathcal{U}_{Y_1} \leftrightarrow \mathcal{U}_{1b}, \quad \mathcal{U}_{CM} \leftrightarrow \mathcal{U}_{5a}, \quad \mathcal{U}_{MM_N} \leftrightarrow \mathcal{U}_{6b}, \\ \mathcal{U}_W^{(2)} &\leftrightarrow \mathcal{U}_{2d}^{(2)}, \quad \mathcal{U}_{CM}^{(2)} \leftrightarrow \mathcal{U}_{5b}^{(2)}. \end{aligned} \quad (25)$$

None of the coefficients involved in the terms listed in this section have any logarithmic contribution at first order in α [see Eq. (16)]. One can conclude that these terms do not contribute to the order $m\alpha^7 \ln(\alpha)$. Since the nonlogarithmic $m\alpha^7$ -order correction is not considered in the present work, in our numerical calculations we truncate the expressions of all coefficients at zero order in α .

B. Terms contributing at the order $m\alpha^7 \ln(\alpha)$

Contributions at this order stem from spin-dependent coefficients of the NRQED Hamiltonian that depend on $\ln(\alpha)$, i.e., c_{q^2} and c_{Y_2} , and can be derived using perturbation theory as done in [5, 11]. The first contribution is from a transverse photon exchange with the c_{q^2} term on the electron side and a dipole vertex [labeled 2N in Eq. (7) of [5]] on the nucleus side. The corresponding effective potential in momentum space is

$$\begin{aligned} \mathcal{U}_{q^2} &= \left[\frac{ie}{8m^3} \mathbf{q}^2 (\boldsymbol{\sigma} \times \mathbf{q}) \right]^k \left[Z_a e \frac{(\mathbf{P}_a + \mathbf{P}'_a)}{2M_a} \right]^l \\ &\quad \times \left[-\frac{1}{\mathbf{q}^2} \left(\delta^{kl} - \frac{q^k q^l}{\mathbf{q}^2} \right) \right] \\ &= \frac{iZ_a e^2}{16m^3 M_a} (\boldsymbol{\sigma} \times \mathbf{q}) \cdot (\mathbf{P}_a + \mathbf{P}'_a) \\ &= -\frac{iZ_a e^2}{16m^3 M_a} [\mathbf{q} \times (\mathbf{P}_a + \mathbf{P}'_a)] \cdot \boldsymbol{\sigma}. \end{aligned} \quad (26)$$

After Fourier transform, the effective potential in real space is found to be

$$\mathcal{U}_{q^2} = \frac{iZ_a e^2}{8m^3 M_a} [\mathbf{p}_e \times 4\pi \delta(\mathbf{r}_a) \mathbf{P}_a - \mathbf{P}_a \times 4\pi \delta(\mathbf{r}_a) \mathbf{p}_e] \cdot \mathbf{s}_e. \quad (27)$$

The other contribution is due to a Coulomb photon exchange with the c_{Y_2} term on the electron side and a Coulomb vertex [2N in Eq. (7) of [5]] on the nucleus side:

$$\begin{aligned} \mathcal{U}_{Y_2} &= \left[\frac{ie}{8m^4} \boldsymbol{\sigma} \cdot [\mathbf{q} \times (\mathbf{p}' + \mathbf{p})] \mathbf{q}^2 \right] [-Z_a e] \left[\frac{1}{\mathbf{q}^2} \right] \\ &= -\frac{iZ_a e^2}{4m^4} (\mathbf{q} \times \mathbf{p}) \cdot \boldsymbol{\sigma}, \end{aligned} \quad (28)$$

which yields for the real-space effective potential

$$\mathcal{U}_{Y_2} = \frac{iZ_a e^2}{2m^4} [\mathbf{p}_e \times 4\pi \delta(\mathbf{r}_a) \mathbf{p}_e] \cdot \mathbf{s}_e. \quad (29)$$

Both terms contribute to the spin-orbit interaction. The total effective potential of order $m\alpha^7 \ln(\alpha)$ is thus obtained as

$$H_{so(7\ln)} = c_{q^2} \mathcal{U}_{q^2} + c_{Y_2} \mathcal{U}_{Y_2}, \quad (30)$$

where only logarithmic terms are taken into account in the expressions of the coefficients c_{q^2} and c_{Y_2} [Eq. (16)]:

$$c_{q^2} \equiv \frac{4}{3} \frac{\alpha}{\pi} \ln(\alpha^{-2}), \quad c_{Y_2} \equiv -\frac{1}{3} \frac{\alpha}{\pi} \ln(\alpha^{-2}). \quad (31)$$

Note that the nonrecoil term \mathcal{U}_{q^2} had been obtained for an electron in an external potential in [25] (see also [26]), but the recoil term \mathcal{U}_{Y_2} had not been considered so far, to the best of our knowledge. There is also a second-order perturbation term:

$$\Delta E_{so(7\ln)}^B = 2 \langle H_{so} Q (E_0 - H_0)^{-1} Q H_{(5\ln)} \rangle, \quad (32)$$

where

$$H_{(5\ln)} = \alpha^3 \frac{4}{3} \ln(\alpha^{-2}) Z_a \delta(\mathbf{r}_a) \quad (33)$$

is the logarithmic part of the effective Hamiltonian describing leading-order radiative corrections. The total correction to the spin-orbit interaction at this order is

$$\Delta E_{so(7\ln)} = \Delta E_{so(7\ln)}^A + \Delta E_{so(7\ln)}^B, \quad (34)$$

with

$$\Delta E_{so(7\ln)}^A = \langle H_{so(7\ln)} \rangle. \quad (35)$$

From the above discussion of logarithmic terms in the NRQED Hamiltonian coefficients, it is clear that there are no effective potentials contributing to the spin-spin tensor interaction at the order $m\alpha^7 \ln(\alpha)$. The only contribution is thus the second-order term

$$\Delta E_{ss(7\ln)}^{(2)} = 2 \langle H_{ss}^{(2)} Q (E_0 - H_0)^{-1} Q H_{(5\ln)} \rangle. \quad (36)$$

The explicit expressions of corrections to the spin-orbit and spin-spin tensor coefficients, which in the H_2^+ case are denoted by c_e and d_1 respectively [see Eq. (3) of [9] for definitions], in terms of reduced matrix elements of the effective potentials listed in this section, are given in Appendix A (see [27] for details).

IV. NUMERICAL RESULTS

A. Variational method

The main features of our numerical method have been described in Ref. [5]. The wave function for a rovibrational state (v, L) is expanded in terms of exponentials of interparticle distances in the following way:

$$\begin{aligned} \Psi_0(\mathbf{R}, \mathbf{r}_1) &= \sum_{l_1+l_2=L} \mathcal{Y}_{LM}^{l_1 l_2}(\hat{\mathbf{R}}, \hat{\mathbf{r}}_1) G_{l_1 l_2}(R, r_1, r_2), \\ \mathcal{Y}_{LM}^{l_1 l_2}(\hat{\mathbf{R}}, \hat{\mathbf{r}}_1) &= R^{l_1} r_1^{l_2} \{Y_{l_1}(\hat{\mathbf{R}}) \otimes Y_{l_2}(\hat{\mathbf{r}}_1)\}_{LM}, \\ G_{l_1 l_2}(R, r_1, r_2) &= \sum_{n=1}^{N/2} \{C_n \operatorname{Re}[e^{-\alpha_n R - \beta_n r_1 - \gamma_n r_2}] \\ &\quad + D_n \operatorname{Im}[e^{-\alpha_n R - \beta_n r_1 - \gamma_n r_2}]\}, \end{aligned} \quad (37)$$

with $\mathbf{R} = \mathbf{R}_2 - \mathbf{R}_1$. The complex exponents α_n , β_n , γ_n are generated in a pseudorandom way in several intervals, which play the role of variational parameters. We have used two intervals for the lower vibrational states ($0 \leq v \leq 4$) and four for higher states ($5 \leq v \leq 9$).

TABLE I. Convergence of the reduced matrix elements involved in the first-order terms \mathcal{U}_W and \mathcal{U}_{Y_1} [Eq. (18)] for the ($L = 1, v = 4$) state of H_2^+ (values are given in a.u.).

N	$p_e^2 \frac{1}{r_1^3} [\mathbf{r}_1 \times \mathbf{p}_e]$	$p_e^2 \frac{1}{r_2^3} [\mathbf{r}_2 \times \mathbf{p}_e]$	$p_e^2 \frac{1}{r_1^3} [\mathbf{r}_1 \times \mathbf{P}_1]$	$p_e^2 \frac{1}{r_2^3} [\mathbf{r}_2 \times \mathbf{P}_2]$
1400	-0.209756[-03]	-0.211145[-03]	-0.718198	-0.718358
1600	-0.211462[-03]	-0.212048[-03]	-0.718194	-0.718138
1800	-0.210752[-03]	-0.210806[-03]	-0.718136	-0.718143
2000	-0.210069[-03]	-0.211858[-03]	-0.718145	-0.718142
2200	-0.210909[-03]	-0.210218[-03]		
2400	-0.211099[-03]	-0.211191[-03]		
2600	-0.211024[-03]	-0.211042[-03]		

B. Second-order terms

Second-order terms have a general expression of the type $\langle AQ(E_0 - H_0)^{-1}QB \rangle$. They are evaluated by solving numerically the equation

$$(E_0 - H_0)\psi^{(1)} = (B - \langle B \rangle)\psi_0, \quad (38)$$

and calculating the scalar product $\langle \Psi_0 | A | \psi^{(1)} \rangle$. In order to solve Eq. (38), $\psi^{(1)}$ is expanded in an ‘‘intermediate’’ variational basis following Eq. (37). As discussed in [5], the most difficult contributions for numerical evaluation are the singular second-order terms: ΔE_{so-H_B} [Eq. (19)], ΔE_{ss-H_B} , [Eq. (23)], $\Delta E_{so(7\ln)}^B$ [Eq. (32)], and $\Delta E_{ss(7\ln)}^{(2)}$ [Eq. (36)]. Indeed, if $B = H_B$ or $B = H_{(5\ln)}$ in Eq. (38), the intermediate wave function $\psi^{(1)}$ behaves like $1/r_1$ ($1/r_2$) at small electron-nucleus distances, resulting in very slow convergence. To circumvent this problem, we rewrite the second-order energy shift as [5]

$$\begin{aligned} & \langle AQ(E_0 - H_0)^{-1}QB \rangle \\ &= \langle AQ(E_0 - H_0)^{-1}QB' \rangle + \langle UA \rangle - \langle U \rangle \langle A \rangle, \end{aligned} \quad (39)$$

where

$$\begin{aligned} U &= \frac{c_1}{r_1} + \frac{c_2}{r_2}, \\ B' &= B - (E_0 - H_0)U - U(E_0 - H_0). \end{aligned} \quad (40)$$

For the case $B = H_B$, we have

$$c_a = \frac{\mu_a(2\mu_a - m_e)}{4m_e^3} Z_a, \quad (41)$$

with $\mu_a = M_a m_e / (M_a + m_e)$, and for $B = H_{(5\ln)}$,

$$c_a = \alpha^3 \frac{4}{3} \ln(\alpha^{-2}) Z_a \times \left(-\frac{\mu_a Z_a}{2\pi} \right). \quad (42)$$

The replacement of B by B' in Eq. (38) reduces the singularity of the intermediate wavefunction. The remaining logarithmic singularity $\psi^{(1)} \sim \ln(r_1)$ [$\ln(r_2)$] still slows the convergence, and necessitates expanding $\psi^{(1)}$ in a ‘‘multilayer’’ basis set (see Table I in [5] for an example), where the first subsets (between 2 and 4) approximate the regular part, and eight additional subsets contain growing exponents β_n (γ_n) up to 10^4 in order to reproduce the singular behavior.

C. Convergence study

We now analyze the convergence of our numerical results. For first-order terms, sufficient accuracy is quite easily ob-

tained; for illustration, the reduced matrix elements involved in calculation of \mathcal{U}_W and \mathcal{U}_{Y_1} [Eq. (18)] are shown in Table I. It is worth noting that the expectation values in columns 2 and 3 (as well as 4 and 5) are not found to be exactly equal in our numerical calculations, as they should be due to the symmetry of the problem with respect to the exchange of nuclei. This is because the permutation symmetry is not explicitly implemented in our basis functions, which would be difficult to do with our choice of coordinates (\mathbf{R}, \mathbf{r}_1) [Eq. (37)]. The observed asymmetries provide a useful cross-check of the precision of our results. Convergence is slower for the terms involving $(\mathbf{r}_a \times \mathbf{p}_e)$, which are related to the electronic contribution to the total orbital momentum, because their nonzero value entirely comes from the smaller ‘‘non- σ ’’ [i.e., $l_2 \neq 0$ in Eq. (37)] components of the wave function. For the same reason, these matrix elements are smaller than those involving $(\mathbf{r}_a \times \mathbf{P}_a)$ by a factor of order $m/M_a \sim 10^{-3}$. Overall, first-order terms are obtained with at least three or four significant digits of accuracy.

Second-order terms, especially the singular terms discussed above, require heavier numerical calculations. This is illustrated in Table II, which shows the convergence of ΔE_{so-H_B} [Eq. (19)]. The quantities appearing in this table are

$$A_a = \left\langle vL \left\| \frac{1}{r_a^3} (\mathbf{r}_a \times \mathbf{p}_e) Q (E_0 - H_0)^{-1} Q H'_B \right\| vL \right\rangle, \quad (43)$$

where H'_B is the effective Hamiltonian obtained by applying the transformation (40) to $B = H_B$, whereas the left-hand side appears in the nonrecoil part of H_{so} [Eq. (20)]. From Table II it can be estimated that these matrix elements are obtained with three significant digits. Second-order matrix elements involving $(\mathbf{r}_a \times \mathbf{P}_a)$ in the left-hand side, corresponding to the recoil part of H_{so} , exhibit faster convergence (not shown in Table II), similarly to what was discussed for first-order terms. A term that deserves a separate discussion, $\Delta E_{so-so}^{(1)}$ [Eq. (19)], is also shown in Table II. Again, only the contributions from the nonrecoil part of H_{so} , which are the most difficult to converge, are shown. These contributions, denoted by a_0^e and a_+^e , are obtained from Eq. (A6) by replacing \mathbf{A}_{so} with \mathbf{A}_{so}^e , which includes only the first term of H_{so} :

$$\mathbf{A}_{so}^e = \frac{Z_a}{2m^2} \frac{(\mathbf{r}_a \times \mathbf{p}_e)}{r_a^3}. \quad (44)$$

The corresponding contribution to c_e is [see Eq. (A5)]

$$\Delta c_e^{(6)}|_{so^e-so^e} = -\frac{1}{2} \frac{1}{L(L+1)} [(L+1)a_-^e + a_0^e - La_+^e]. \quad (45)$$

TABLE II. Convergence of second-order terms contributing to ΔE_{so-H_B} and to $\Delta E_{so-so}^{(1)}$ for the ($L = 1, v = 4$) state of H_2^+ (values are given in a.u.).

N	A_1	A_2	a_0^e	a_+^e	$\Delta c_e^{(6)} _{so-so}$
8000	-0.746134[-04]	-0.801218[-04]	-0.12654393[-01]	-0.12680066[-01]	-0.6418[-05]
10 000	-0.795165[-04]	-0.797075[-04]	-0.12657847[-01]	-0.12680231[-01]	-0.5596[-05]
12 000	-0.796812[-04]	-0.797663[-04]	-0.12657987[-01]	-0.12680252[-01]	-0.5566[-05]
14 000	-0.796931[-04]	-0.797285[-04]	-0.12658040[-01]	-0.12680278[-01]	-0.5560[-05]
16 000	-0.797234[-04]	-0.797646[-04]	-0.12658073[-01]	-0.12680294[-01]	-0.5555[-05]

As can be seen from Table II, the quantities a_0^e, a_+^e converge more rapidly than A_1 and A_2 , in accordance with the fact that H_{so} is less singular than H'_B . However, due to a quasicancellation between the different angular momentum components, they are larger than the total contribution $\Delta c_e^{(6)}|_{so-so}$ by several orders of magnitude. As a consequence, they need to be calculated with a high relative accuracy, which requires using a large variational basis. From the results of Table II, the numerical uncertainty of $\Delta c_e^{(6)}|_{so-so}$ may be conservatively estimated to $10^{-7} E_h \alpha^4$ (where E_h is the Hartree energy), i.e., less than 2 Hz.

D. Results

The values of all the contributions to the spin-orbit coefficient c_e are given in Table III for a few states of interest for experiments. Note that the term \mathcal{U}_{MM_N} [Eq. (18)] was omitted, because it was found to be smaller than 1 Hz, which is negligible with respect to the overall uncertainty. Our theoretical values of c_e can be found in the last column. Complete results for the rovibrational states ($0 \leq L \leq 4, 0 \leq v \leq 9$) are given in the Supplemental Material [28].

The numerical uncertainty is dominated by the singular second-order term ΔE_{so-H_B} ; from the convergence study shown in the previous paragraph and similar tests performed for higher vibrational states, it is estimated to be smaller than 10 Hz for all rovibrational states. The theoretical uncertainty is mainly due to the yet uncalculated nonlogarithmic correction of order $m\alpha^7$ [26,29]. We estimate it to about one third of the $m\alpha^7 \ln(\alpha)$ correction, which corresponds to 100–150 Hz or 3–4 ppm.

TABLE III. Corrections to the spin-orbit interaction coefficient c_e for a few rovibrational states of H_2^+ (in kHz). The leading-order (Breit-Pauli) value $c_e^{(BP)}$ (Ref. [9]) is given in column 2. Columns 3–5 and 6–8 are respectively the first-order and second-order contributions [Eqs. (18) and (19)] at the $m\alpha^6$ order, and the total correction at this order, $\Delta c_e^{(6)}$, is given in column 9. Columns 10–12 are the first-order [Eqs. (35) and 30] and second-order [Eq. (32)] contributions at the $m\alpha^7 \ln(\alpha)$ order, respectively. The total correction at this order, $\Delta c_e^{(7\ln)}$, is given in column 13. The last column is our value of c_e . Its estimated uncertainty (equal to one third of $\Delta c_e^{(7\ln)}$) is indicated between parentheses.

(L, v)	$c_e^{(BP)}$	\mathcal{U}_{Y_1}	\mathcal{U}_W	\mathcal{U}_{CM}	ΔE_{so-H_B}	$\Delta E_{so-so}^{(1)}$	ΔE_{so-ret}	$\Delta c_e^{(6)}$	\mathcal{U}_{Y_1}	\mathcal{U}_{q_2}	$\Delta E_{so-H(5\ln)}$	$\Delta c_e^{(7\ln)}$	c_e (this work)
(1,0)	42 416.318	1.551	-3.631	0.028	2.765	0.414	0.333	1.460	-0.035	0.060	-0.486	-0.460	42 417.32(15)
(1,4)	32 654.638	1.205	-2.979	0.055	2.154	0.325	0.261	1.020	-0.027	0.049	-0.364	-0.342	32 655.32(11)
(1,5)	30 437.196	1.127	-2.813	0.058	2.010	0.305	0.239	0.925	-0.025	0.046	-0.337	-0.316	30 437.80(11)
(1,6)	28 280.421	1.049	-2.645	0.059	1.858	0.283	0.220	0.824	-0.023	0.044	-0.312	-0.292	28 280.95(10)
(2,0)	42 162.530	1.542	-3.601	0.027	2.733	0.412	0.336	1.447	-0.034	0.060	-0.481	-0.456	42 163.52(15)
(2,1)	39 571.598	1.451	-3.440	0.036	2.579	0.388	0.311	1.326	-0.032	0.057	-0.448	-0.424	39 572.50(14)

Regarding the spin-spin tensor interactions, we write the related term of the H_2^+ effective spin Hamiltonian [9] in the following way:

$$H_{\text{eff}}^{ss(2)} = d_1(2\mathbf{L}^2(\mathbf{s}_e \cdot \mathbf{I}) - 3[(\mathbf{L} \cdot \mathbf{s}_e)(\mathbf{L} \cdot \mathbf{I}) + (\mathbf{L} \cdot \mathbf{I})(\mathbf{L} \cdot \mathbf{s}_e)]) \quad (46)$$

This definition differs from that of Ref. [9] by a factor $3(2L - 1)(2L + 3) = 15$ (for $L = 1$), but coincides with that of the E_6 coefficient in the HD^+ effective spin Hamiltonian [10], which facilitates future comparison between H_2^+ and HD^+ . The values of all the contributions to the d_1 coefficient are given in Table IV for a few $L = 1$ states, whereas complete results for the rovibrational states ($0 \leq L \leq 4, 0 \leq v \leq 9$) are given in the Supplemental Material [28]. The second-order terms $\Delta E_{so-ss}^{(2)}$ and $\Delta E_{so-so_N}^{(2)}$ have been omitted because they were found to be much smaller than the overall uncertainty. The numerical uncertainty, dominated by the singular second-order term $\Delta E_{ss-H_B}^{(2)}$, is estimated to be smaller than 1 Hz for all rovibrational states. Similarly to the spin-orbit coefficient, the theoretical uncertainty due to the yet uncalculated nonlogarithmic correction of order $m\alpha^7$ is estimated to about one third of the $m\alpha^7 \ln(\alpha)$ correction, which corresponds to 10–20 Hz or about 2 ppm.

V. COMPARISON WITH EXPERIMENTS

We now use our values of the c_e and d_1 coefficients to obtain improved theoretical predictions of the hyperfine intervals measured in [19], see Table V. To do this, we diagonalize the effective spin Hamiltonian of Ref. [9]. The

TABLE IV. Corrections to the spin-spin tensor interaction coefficient d_1 for a few rovibrational states of H_2^+ (in kHz). The leading-order (Breit-Pauli) value $d_1^{(BP)}$ (Ref. [9]) is given in column 2. Columns 3–4 and 5 are respectively the first-order and second-order contributions [Eqs. (22) and (23)] at the $m\alpha^6$ order. The total correction at this order, $\Delta d_1^{(6)}$, is given in column 6. Column 7 is the second-order contribution at the $m\alpha^7 \ln(\alpha)$ order [Eq. (36)]. The last column is our value for d_1 . Its estimated uncertainty (equal to one third of $\Delta d_1^{(7\ln)}$) is indicated between parentheses. To match the notations of Ref. [9], all values should be multiplied by $3(2L-1)(2L+3) = 15$.

(L, v)	$d_1^{(BP)}$	$\mathcal{U}_W^{(2)}$	$\mathcal{U}_{CM}^{(2)}$	$\Delta E_{ss-H_B}^{(2)}$	$\Delta d_1^{(6)}$	$\Delta d_1^{(7\ln)}$	d_1 (this work)
(1,0)	8565.983	-0.802	0.092	0.951	0.241	-0.050	8566.174(17)
(1,4)	6537.247	-0.642	0.079	0.740	0.178	-0.039	6537.386(13)
(1,5)	6080.287	-0.603	0.076	0.676	0.149	-0.036	6080.400(12)
(1,6)	5637.524	-0.564	0.072	0.629	0.137	-0.033	5637.627(11)

values of the spin-spin contact interaction coefficient b_F are taken from [6]; it is worth recalling that they have been found to be in excellent agreement with experimental rf spectroscopy data [30]. The smaller hyperfine coefficients c_I and d_2 , which respectively describe the nuclear spin-orbit and the proton-proton spin-spin tensor interaction, are calculated in the framework of the Breit-Hamiltonian with account of the electron's anomalous magnetic moment [9]. The values of all the coefficients used here can be found in Table VI (Appendix B).

In order to estimate the uncertainties of the theoretical hyperfine intervals f_v , we calculated the derivatives

$$\gamma_{c_e, v} = \frac{\partial f_v}{\partial c_e}, \quad \gamma_{c_I, v} = \frac{\partial f_v}{\partial c_I}, \quad \dots \quad (47)$$

Their values for the three rovibrational levels of interest are given in Table VII (Appendix C). The uncertainty of f_v is calculated via propagation of the uncertainties of the hyperfine coefficients. Note that this uncertainty only weakly depends on our assumptions regarding correlations, because it is dominated by the uncertainty of the c_e coefficient, whereas the second largest uncertainty, from d_1 , is smaller by more than one order of magnitude. Assuming no correlations between uncertainties of different coefficients, the total uncertainty is

$$u(f_v) = \sqrt{[\gamma_{c_e, v} u(c_e, v)]^2 + [\gamma_{c_I, v} u(c_I, v)]^2 + [\gamma_{b_F, v} u(b_F, v)]^2 + [\gamma_{d_1, v} u(d_1, v)]^2 + [\gamma_{d_2, v} u(d_2, v)]^2}. \quad (48)$$

The uncertainties $u(c_e)$ and $u(d_1)$ have been estimated above, $u(b_F)$ is taken from [6], and for the coefficients calculated at the Breit-Pauli level we take $u(c_I) = \alpha^2 c_I$ and $u(d_2) = \alpha^2 d_2$.

The comparison between theory and experiment, presented in Table V, reveals a reasonable agreement. The observed deviations, which range between 1.2 and 1.6 σ , may for example be caused by a slight underestimate of the nonlogarithmic correction of order $m\alpha^7$ to the spin-orbit coefficient c_e .

In conclusion, we have advanced the hyperfine structure theory in hydrogen molecular ions by calculating higher-order corrections to the spin-orbit and spin-spin tensor interactions. This allowed us to improve the accuracy of the related hy-

TABLE V. Comparison between theory and experiment for the hyperfine splitting between the $(F = 1/2, J = 3/2)$ and $(F = 1/2, J = 1/2)$ states (in MHz). The second column gives the theoretical prediction obtained from calculation of the hyperfine coefficients at the Breit-Pauli level, and the third one is our prediction including higher-order corrections to b_F , c_e , and d_1 . The experimental values are shown in the last column.

(L, v)	Theory [9]	Theory (this work)	Experiment [19]
(1,4)	15.371 0(9)	15.371 316(56)	15.371 407(2)
(1,5)	14.381 2(8)	14.381 453(52)	14.381 513(2)
(1,6)	13.413 2(7)	13.413 397(48)	13.413 460(2)

perine coefficients in H_2^+ by about one order of magnitude and reach agreement with rf spectroscopy data at a level of 4–6 ppm. In the future, the theory can be improved further by calculating nonlogarithmic $m\alpha^7$ -order corrections to the spin-orbit coefficient. Application to HD^+ , which has been a subject of several high-precision experiments in recent years, will be presented in a forthcoming paper.

APPENDIX A: EXPRESSIONS OF CORRECTIONS TO THE HYPERFINE COEFFICIENTS

All the first-order terms contributing to the spin-orbit interaction, Eqs. (18), (35), and (30), as well as the second-order terms ΔE_{so-H_B} , ΔE_{so-ret} in Eq. (19) and $\Delta E_{so(7\ln)}^B$ [Eq. (32)], can be written in the form $\langle \mathcal{U}_i \rangle = \langle \mathbf{A}_i \cdot \mathbf{s}_e \rangle$, where \mathbf{A}_i is a vector operator acting on space variables. The corresponding correction to the spin-orbit coefficient (denoted by c_e in H_2^+ [9]) is then obtained from the Wigner-Eckart theorem as

$$\Delta c_e(v, L) = \frac{\langle vL || \mathbf{A}_i || vL \rangle}{\langle L || \mathbf{L} || L \rangle} = \frac{\langle vL || \mathbf{A}_i || vL \rangle}{\sqrt{L(L+1)(2L+1)}}. \quad (A1)$$

Similarly, the first-order terms contributing to the spin-spin tensor interaction [Eq. (22)], and the second-order terms $\Delta E_{ss-H_B}^{(2)}$ in Eq. (23) and $\Delta E_{ss(7\ln)}^{(2)}$ [Eq. (36)], can be written in the form $\langle \mathcal{U}_i \rangle = \langle \mathbf{T}_i^{(2)} \cdot \mathbf{U}^{(2)} \rangle$, where $\mathbf{T}_i^{(2)}$ is an operator of

TABLE VI. Hyperfine coefficients for a few rovibrational states of H_2^+ (in kHz). The value of b_F (resp. c_I , d_2) is taken from [6] (resp. [9]). Uncertainties are discussed in the main text. To match the notations of Ref. [9], all the d_2 values should be multiplied by $3(2L-1)(2L+3) = 15$.

(L, v)	b_F	c_I	d_2
(1,4)	836 728.705	-35.826	-16.414
(1,5)	819.226 705	-34.148	-15.531
(1,6)	803 174.518	-32.385	-14.633

rank 2 acting on space variables, and (see Appendix B in [5])

$$\mathbf{U}_\mu^{(2)} = \{\mathbf{s}_e \otimes \mathbf{I}\}_\mu^{(2)} = \sqrt{\frac{3}{2}} \left[\frac{1}{2} (s_e^i I^j + s_e^j I^i) - \frac{\delta^{ij}}{3} (\mathbf{s}_e \cdot \mathbf{I}) \right]_\mu^{(2)}. \quad (\text{A2})$$

Here $\mathbf{I} = \mathbf{I}_1 + \mathbf{I}_2$ is the total nuclear spin. Using again the Wigner-Eckart theorem and the relationship

$$\begin{aligned} (\mathbf{L} \otimes \mathbf{L})^{(2)} \cdot (\mathbf{s}_e \otimes \mathbf{I})^{(2)} \\ = \frac{1}{2} \sqrt{\frac{3}{2}} \left[(\mathbf{L} \cdot \mathbf{s}_e)(\mathbf{L} \cdot \mathbf{I}) + (\mathbf{L} \cdot \mathbf{I})(\mathbf{L} \cdot \mathbf{s}_e) - \frac{2}{3} \mathbf{L}^2 (\mathbf{s}_e \cdot \mathbf{I}) \right], \end{aligned} \quad (\text{A3})$$

one gets for the correction to the tensor coefficient (denoted by d_1 in H_2^+ [9])

$$\begin{aligned} \Delta d_1(v, L) &= -\frac{1}{2\sqrt{6}} \frac{\langle vL || \mathbf{T}_i^{(2)} || vL \rangle}{\langle L || (\mathbf{L} \otimes \mathbf{L})^{(2)} || L \rangle} \\ &= -\frac{\langle vL || \mathbf{T}_i^{(2)} || vL \rangle}{2\sqrt{L(L+1)(2L-1)(2L+1)(2L+3)}}. \end{aligned} \quad (\text{A4})$$

Some of the second-order terms are more complicated because they involve a coupling of two spatial operators of rank 1 or 2. This case was treated in detail in the Appendix B of [5]; we give here only the final formula for the term $\Delta E_{so-so}^{(1)}$ in Eq. (19), as obtained by applying Eqs. (B3) and (B6) of that reference:

$$\Delta c_e(v, L) = -\frac{1}{2} \frac{1}{L(L+1)} [(L+1)a_- + a_0 - La_+], \quad (\text{A5})$$

TABLE VII. Derivatives of the interval between the ($F = 1/2, J = 3/2$) and ($F = 1/2, J = 1/2$) states for three rovibrational levels of H_2^+ .

(L, v)	$\gamma_{c_e, v}$	$\gamma_{c_I, v}$	$\gamma_{b_F, v}$	$\gamma_{d_1, v}$	$\gamma_{d_2, v}$
(1,4)	0.488	-1.989	0.0013	-0.266	0.257
(1,5)	0.489	-1.990	0.0012	-0.252	0.244
(1,6)	0.490	-1.991	0.0011	-0.238	0.230

where

$$\begin{aligned} a_- &= -\frac{1}{2L+1} \sum_{n \neq 0} \frac{\langle vL || \mathbf{A}_{so} || v_n L - 1 \rangle \langle v_n L - 1 || \mathbf{A}_{so} || vL - 1 \rangle}{E_0 - E_n}, \\ a_0 &= \frac{1}{2L+1} \sum_{n \neq 0} \frac{\langle vL || \mathbf{A}_{so} || v_n L \rangle \langle v_n L || \mathbf{A}_{so} || vL \rangle}{E_0 - E_n}, \\ a_+ &= -\frac{1}{2L+1} \sum_{n \neq 0} \frac{\langle vL || \mathbf{A}_{so} || v_n L + 1 \rangle \langle v_n L + 1 || \mathbf{A}_{so} || vL + 1 \rangle}{E_0 - E_n}. \end{aligned} \quad (\text{A6})$$

\mathbf{A}_{so} is the spatial part of the spin-orbit Hamiltonian H_{so} in Eq. (20), i.e. $H_{so} = \mathbf{A}_{so} \cdot \mathbf{s}_e$.

APPENDIX B: OTHER COEFFICIENTS OF THE EFFECTIVE SPIN HAMILTONIAN

We give in Table VI the values of all the coefficients of the H_2^+ effective spin Hamiltonian (see Eq. (3) of [9]) in the three rovibrational states for which theoretical hyperfine intervals are calculated and compared with experimental data (see Table V).

APPENDIX C: DERIVATIVES OF HYPERFINE INTERVALS WITH RESPECT TO THE HYPERFINE COEFFICIENTS

We give in Table VII the values of the derivatives $\gamma_{c_e, v}$, $\gamma_{c_I, v}$, ... (as defined in Eq. (47)) for the same three rovibrational states. These quantities are required to estimate the uncertainties of theoretical hyperfine intervals (see Eq. (48)).

- [1] S. Alighanbari, G. S. Giri, F. L. Constantin, V. I. Korobov, and S. Schiller, Precise test of quantum electrodynamics and determination of fundamental constants with HD^+ ions, *Nature (London)* **581**, 152 (2020).
- [2] S. Patra, M. Germann, J.-Ph. Karr, M. Haidar, L. Hilico, V. I. Korobov, F. M. J. Cozijn, K. S. E. Eikema, W. Ubachs, and J. C. J. Koelemeij, Proton-electron mass ratio from laser spectroscopy of HD^+ at the part-per-trillion level, *Science* **369**, 1238 (2020).
- [3] V. I. Korobov and J.-Ph. Karr, Rovibrational spin-averaged transitions in the hydrogen molecular ions, *Phys. Rev. A* **104**, 032806 (2021).
- [4] M. Germann, S. Patra, J.-Ph. Karr, L. Hilico, V. I. Korobov, E. J. Salumbides, K. S. E. Eikema, W. Ubachs, and J. C. J.

Koelemeij, Three-body QED test and fifth-force constraint from vibrations and rotations of HD^+ , *Phys. Rev. Research* **3**, L022028 (2021).

- [5] V. I. Korobov, J.-Ph. Karr, M. Haidar, and Z.-X. Zhong, Hyperfine structure in the H_2^+ and HD^+ molecular ions at order ma^6 , *Phys. Rev. A* **102**, 022804 (2020).
- [6] J.-Ph. Karr, M. Haidar, L. Hilico, Z.-X. Zhong, and V. I. Korobov, Higher-order corrections to spin-spin scalar interactions in HD^+ and H_2^+ , *Phys. Rev. A* **102**, 052827 (2020).
- [7] J. C. J. Koelemeij, Effect of correlated hyperfine theory errors in the determination of rotational and vibrational transition frequencies in HD^+ , *J. Mol. Spectrosc.* e2058637 (2022).
- [8] V. I. Korobov, J. C. J. Koelemeij, L. Hilico, and J.-Ph. Karr, Theoretical Hyperfine Structure of the Molecular

- Hydrogen Ion at the 1 ppm Level, *Phys. Rev. Lett.* **116**, 053003 (2016).
- [9] V. I. Korobov, L. Hilico, and J.-Ph. Karr, Hyperfine structure in the hydrogen molecular ion, *Phys. Rev. A* **74**, 040502(R) (2006).
- [10] D. Bakalov, V. I. Korobov, and S. Schiller, High-Precision Calculation of the Hyperfine Structure of the HD^+ Ion, *Phys. Rev. Lett.* **97**, 243001 (2006).
- [11] M. Haidar, Z.-X. Zhong, V.-I. Korobov, and J.-Ph. Karr, Non-relativistic QED approach to the fine- and hyperfine-structure corrections of order $m\alpha^6$ and $m\alpha^6(m/M)$: Application to the hydrogen atom, *Phys. Rev. A* **101**, 022501 (2020).
- [12] C.-W. Chou, C. Kurz, D. B. Hume, P. N. Plessow, D. R. Leibbrandt, and D. Leibfried, Preparation and coherent manipulation of pure quantum states of a single molecular ion, *Nature (London)* **545**, 203 (2017).
- [13] J. Schmidt, T. Louvradoux, J. Heinrich, N. Sillitoe, M. Simpson, J.-Ph. Karr, and L. Hilico, Trapping, Cooling, and Photodissociation Analysis of State-Selected H_2^+ Ions Produced by $(3 + 1)$ Multiphoton Ionization, *Phys. Rev. Appl.* **14**, 024053 (2020).
- [14] B. Tu, F. Hahne, I. Arapoglou, A. Egl, F. Heiße, M. Höcker, C. König, J. Morgner, T. Sailer, A. Weigel *et al.*, Tank-circuit assisted coupling method for sympathetic laser cooling, *Adv. Quantum Technol.* **4**, 2100029 (2021).
- [15] K. B. Jefferts, A. A. Penzias, K. A. Ball, D. F. Dickinson, and A. E. Lilley, Radio search for interstellar H_2^+ , *Astrophys. J.* **159**, L15 (1970).
- [16] W. L. H. Shuter, D. R. W. Williams, S. R. Kulkarni, and C. Heiles, A search for vibrationally excited interstellar H_2^+ , *Astrophys. J.* **306**, 255 (1986).
- [17] J. H. Black, Molecules in harsh environments, *Faraday Discuss.* **109**, 257 (1998).
- [18] E. G. Myers, *CPT* tests with the antihydrogen molecular ion, *Phys. Rev. A* **98**, 010101(R) (2018).
- [19] S. C. Menasian and H. G. Dehmelt, High-resolution study of $(1, 1/2, 1/2)$ - $(1, 1/2, 3/2)$ HFS transitions in H_2^+ , *Bull. Am. Phys. Soc.* **18**, 408 (1973).
- [20] T. Kinoshita and M. Nio, Radiative corrections to the muonium hyperfine structure: The $\alpha^2(Z\alpha)$ correction, *Phys. Rev. D* **53**, 4909 (1996).
- [21] A. V. Manohar, Heavy quark effective theory and nonrelativistic QCD Lagrangian to order α_s/m^3 , *Phys. Rev. D* **56**, 230 (1997).
- [22] R. J. Hill, G. Lee, G. Paz, and M. P. Solon, NRQED Lagrangian at order $1/M^4$, *Phys. Rev. D* **87**, 053017 (2013).
- [23] M. Nio and T. Kinoshita, Radiative corrections to the muonium hyperfine structure. II. The $\alpha(Z\alpha)^2$ correction, *Phys. Rev. D* **55**, 7267 (1997).
- [24] P. Labelle and S. M. Zebarjad, Derivation of the Lamb shift using an effective field theory, *Can. J. Phys.* **77**, 267 (1999).
- [25] U. D. Jentschura, A. Czarnecki, and K. Pachucki, Nonrelativistic QED approach to the Lamb shift, *Phys. Rev. A* **72**, 062102 (2005).
- [26] K. Pachucki, Quantum electrodynamics effects on helium fine structure, *J. Phys. B: At. Mol. Opt. Phys.* **32**, 137 (1999).
- [27] M. Haidar, PhD. thesis, Sorbonne Université (2021).
- [28] See Supplemental Material at <http://link.aps.org/supplemental/10.1103/PhysRevA.106.022816> for numerical results on the spin-orbit and spin-spin tensor coefficients for a range of rovibrational states in H_2^+ .
- [29] K. Pachucki and V. A. Yerokhin, Reexamination of the helium fine structure, *Phys. Rev. A* **79**, 062516 (2009).
- [30] K. B. Jefferts, Hyperfine Structure in the Molecular Ion H_2^+ , *Phys. Rev. Lett.* **23**, 1476 (1969).